Mediated Electronic Coupling: Singlet Energy Transfer in Porphyrin Dimers Enhanced by the Bridging Chromophore

Kristine Kilså,[†] Johan Kajanus,[‡] Jerker Mårtensson,[‡] and Bo Albinsson*,[†]

Department of Physical Chemistry and Department of Organic Chemistry, Chalmers University of Technology, SE−412 96 Göteborg Sweden

Received: March 15, 1999; In Final Form: June 2, 1999

We have studied singlet electronic energy transfer (EET) in two donor−bridge−acceptor series (D−B−A), in which the donor (zinc porphyrin or its pyridine complex) and the acceptor (free base porphyrin) were covalently connected by a geometrically well-defined bridging chromophore. We have investigated how the medium between a donor and an acceptor influences EET by separating the influence of the electronic structure of the bridging chromophore from other effects known to influence the energy transfer. The electronic structure of the bridging chromophore was varied by changing the central unit (bicyclo[2.2.2]octane, benzene, naphthalene, or anthracene) in the bridging chromophore. In all systems the excited state energy separation donor-bridge and bridge-acceptor is large enough to prevent stepwise singlet energy transfer. In addition, the systems were designed to minimize conjugation to preserve the identity of the separate chromophores (donor, bridge, acceptor). Compared with the rate constant expected from the Förster theory, the bridging chromophore with bicyclo[2.2.2]octane as the central unit did not significantly enhance the energy transfer rate constant. However, the bridging chromophores with benzene and naphthalene as the central unit showed a moderate increase, whereas the bridging chromophore with anthracene as the central unit showed the largest increase in energy transfer rate constant. This increase is ascribed to a mediating effect of the bridging chromophore and it is proposed to be strongly correlated to the energy splitting between the singlet excited states of donor and bridging chromophores.

Introduction

Knowledge of the factors that govern energy and electron-transfer processes is crucial to our understanding of natural photosynthesis and many other biological processes.[1] It will also be important for the future construction of artificial photosynthetic complexes[2] and molecular photonic or electronic devices.[3] The electronic coupling between a donor and an acceptor that underlies energy and electron transfer processes has been studied intensively with respect to different factors that affect its magnitude.[4] The magnitude of the coupling determines the rate of the transfer process. One of the factors that influence electronic coupling is the electronic structure of the medium between the donor and the acceptor. The intervening medium may be a protein scaffold, as where the natural transfer processes occur. It may also be solvent molecules or a bridge covalently linking the donor and acceptor, as found in most artificial systems. The effect of the medium between donor and acceptor can be studied in donor−bridge−acceptor (D−B−A) systems in which the three parts can be regarded as individual chromophores. The bridging chromophore, in addition to acting as an intervening medium, serves as a spacer between donor and acceptor and provides geometrical constraints on the system. Furthermore, the bridging chromophore can be changed to either "insulate" or "conduct", thus enabling its effect on the transfer processes to be studied.

Electronic energy transfer (EET) is often described as caused by either an orbital overlap-dependent exchange coupling *or* a Coulomb coupling, even though they act in conjunction. The former short-range orbital-dependent coupling has been mediated over relatively large D−A distances by the bonds in the intervening medium, i.e., the bridge.[5] Closs et al.[6] first demonstrated that a bridge with only σ-bonds could promote triplet−triplet EET analogously to promotion of electron transfer.[7] A marked rate dependence on the conformations of the σ-bonds was also found for the studied isomers, which indicates through-bond electronic coupling.[7,8] These observations of EET mediated through σ-bonds have been confirmed and similar results concerning singlet−singlet EET have been reported in several recent publications.[9] The theoretical treatment[10] of such systems is based on the through-bond mechanism used to explain intramolecular electron transfer.[11] Other issues that have been addressed experimentally are the distance dependence on the EET rate in D−B−A systems in which the bridge has a large conjugated π-electronic system,[12] and the dependence on the point of attachment of the bridge at the D and A.[13]

The Coulomb coupling may occur over large distances without mediation because no orbital overlap is required. However, it also has been suggested that this coupling may be relayed by the intervening medium.[9e,14] As the energy of the lowest excited electronic state of the bridge approaches that of the donor excited state it is expected to become increasingly important as a mediating channel. Nevertheless, to the best of our knowledge, a systematic study of the EET rate dependence on the energy of the lowest excited state of such bridges has not yet been reported. The diversity of features of the intervening medium that influences the transfer processes makes it one of

* To whom correspondence should be addressed.
[†] Department of Physical Chemistry.
[‡] Department of Organic Chemistry.

10.1021/jp9909098 CCC: $18.00
Published on Web 08/05/1999

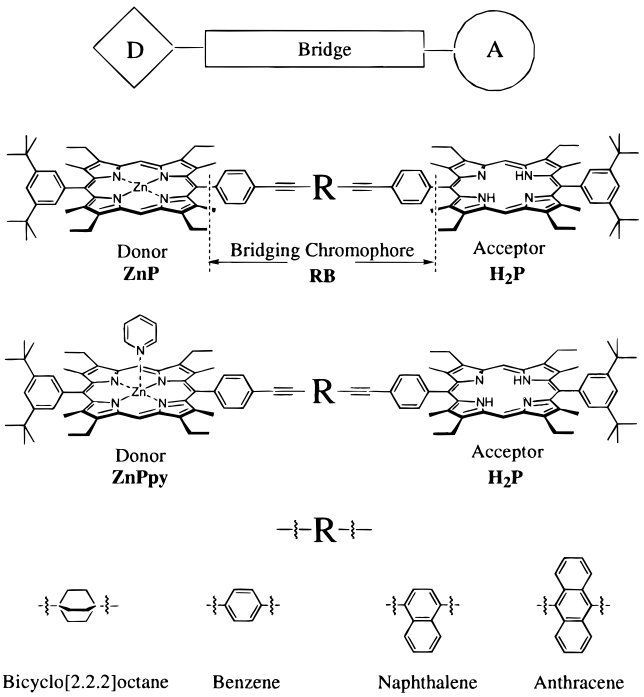

Figure 1. Structure of the studied donor−bridge−acceptor systems. The dimers are denoted ZnP−RB−H_2P and the corresponding reference compounds are denoted ZnP−RB and RB−H_2P. With pyridine as an axial ligand to zinc porphyrin the donor is changed to ZnPpy. RB is the bridging chromophore, where R is the central unit, which is either bicyclo[2.2.2]octane (O), benzene (B), naphthalene (N), or anthracene (A).

the least understood factors controlling energy and electron transfer, yet it is important because of its potential use in the future design of supramolecular systems to control and optimize the transfer processes.

Preliminary results[15] have shown that in a series of porphyrin dimers, the energy transfer rate constant, k_{EET}, increased with decreasing energy level of the lowest singlet excited state of the aromatic bridging chromophore. This article presents full experimental details for an extended number of D−B−A systems accompanied by a qualitative analysis of the bridge mediating effect. The systems consist of porphyrin moieties covalently linked by a rigid bridging chromophore and the three parts can be regarded as individual chromophores. In both series the electronic structure of the bridging chromophore is varied, whereas variations in all other parameters known to influence EET have been minimized carefully.

Results

The general structure of the studied D−B−A systems is shown in Figure 1. We have synthesized and investigated two series of porphyrin dimers in which the central unit in the bridging chromophore has been varied. The electronic structure is hereby varied and hence the energy of the lowest singlet excited state of the bridging chromophore. Three of the four bridging chromophores are fully conjugated systems; bis-(phenylethynyl)arylene where the central arylene is either 1,4-phenylene (BB), 1,4-naphthylene (NB), or 9,10-anthrylene (AB). In the fourth bridging chromophore the conjugation is broken by substitution of the arylene by 1,4-bicyclo[2.2.2]octylene (OB). In both series the acceptor is 5,15-diphenyl-α,β-octaalkyl porphyrin (H_2P), whereas the donor is either the corresponding zinc porphyrin (ZnP) or its pyridine complex (ZnPpy) (Figure 1).

Design. We have constructed the D−B−A systems to answer questions about the influence of the medium between donor and acceptor on the EET process. Therefore, the design of the series of systems was such that variation in all other parameters known to affect the EET process was minimized. The systems were designed based on the following criteria: (i) The distance between the donor and the acceptor should be constant throughout the series. (ii) The relative orientation of the donor and the acceptor should be independent of the bridging chromophore. (iii) Simple π-conjugation through the system should be avoided to preserve the identity of the donor, bridge, and acceptor chromophores.

Structure. The design criteria are met in the investigated systems. (i) Quantum mechanical calculations (Table 1) show that the length of the bridging chromophore is, within the accuracy of the methods used, equal for all four bridging chromophores, 16.4 Å. Furthermore, the length of the bridging chromophore does not depend on the orientation of the central unit relative to the plane of the phenyl groups. Thus, the distance between donor and acceptor is equal in all systems. From the MM+[16] optimized structure of ZnP−BB−H_2P, a center-to-center distance of 25.3 Å was estimated.[15] (ii) The angular distribution between the porphyrin planes and the central unit are almost uniform because of the use of the triple bonds in the bridging chromophore (Figure 1). The rotational barrier of the central unit was investigated by keeping the phenyl groups in one plane and rotating the central unit around the triple bonds, thereby changing the dihedral angle (α) between the central unit and the plane of the phenyl groups. The structures were optimized and the energy calculated at fixed angles (0°, 15°... 90°). The largest rotational barrier (0.82 kcal/mol at $\alpha = 90°$) was found for AB using PM3[17] (Table 1) whereas ab initio (HF/3-21G*)[18] calculations gave a smaller barrier for AB and the largest for BB (0.96 kcal/mol). The low barriers show that at room temperature all relative orientations of the porphyrin planes are energetically attainable and that a rapid interconversion between different conformations is to be expected. (iii) Conjugation through the system is minimized as judged by the conservation of the absorption spectra of the D−B−A systems compared with its components (vide infra). The methyl groups in the β-position of the porphyrin moieties (next to the phenyl groups) force the porphyrin and phenyl planes to be almost orthogonal because of steric encumbrance. The angular deviation from orthogonality at room temperature was estimated computationally by varying the dihedral angle between the porphyrin and phenyl planes (90°, 85° ... 55°) in H_2P, optimizing the structure, and calculating the potential energy at these fixed dihedral angles (PM3). In this way, the span of the dihedral angle between the planes of the porphyrin and the adjacent phenyl group was estimated to be $90° \pm 22°$ at room temperature (90% of the conformers according to the Boltzmann distribution).

Synthesis. The D−B−A systems were assembled using a building block approach with a palladium-catalyzed cross-coupling reaction (Sonogashira coupling).[19,20] The syntheses of ZnP, H_2P, the arene-linked porphyrin dimers, and corresponding reference compounds are presented elsewhere.[21]

The formally nonconjugated porphyrin dimer ZnP−OB−H_2P was prepared from zinc iodoporphyrin **8**,[21] free base iodoporphyrin **11**,[21] and a bicyclo[2.2.2]octane building block **5** (Scheme 2). Diyne **5** was monosilylated, so that the two porphyrins in different states of metalation could be introduced in a stepwise manner. The reference compounds ZnP−OB and OB−H_2P, and the bridging chromophore 1,4-bis(phenylethynyl)-

TABLE 1: Calculated Relative Energies and Distances for Different Dihedral Angles in the Bridging Chromophores

bridging chromophore	α,[a] deg	AM1		PM3		HF/3-21G*	
		distance,[b] Å	energy,[c] kcal mol^{-1}	distance,[b] Å	energy,[c] kcal mol^{-1}	distance,[b] Å	energy,[c] kcal mol^{-1}
OB	0	16.3	0.00	16.3	0.00	16.3	0.00
OB	90	16.3	0.00	16.3	0.00	16.3	0.00
BB	0	16.4	0.00	16.4	0.00	16.5	0.00
BB	90	16.4	0.45	16.4	0.48	16.5	0.96
NB	0	16.4	0.00	16.4	0.00	16.5	0.00
NB	90	16.4	0.36	16.4	0.58	16.5	0.66
AB	0	16.5	0.00	16.4	0.00	16.5	0.00
AB	90	16.5	0.34	16.4	0.82	16.5	0.35

[a] Orientation of the plane of the central unit relative to the plane of the adjacent phenyls. α = 0° corresponds to both phenyl groups and the central chromophore in the same plane. For bicyclo[2.2.2]octane, α = 0° corresponds to both phenyls and one of the three vertical symmetry planes of bicyclo[2.2.2]octance in the same plane. [b] Length of the bridging chromophore (between the *para*-carbons of the phenyl groups). [c] Energy of the bridging chromophore relative to the global minimum at α = 0°.

SCHEME 1[a]

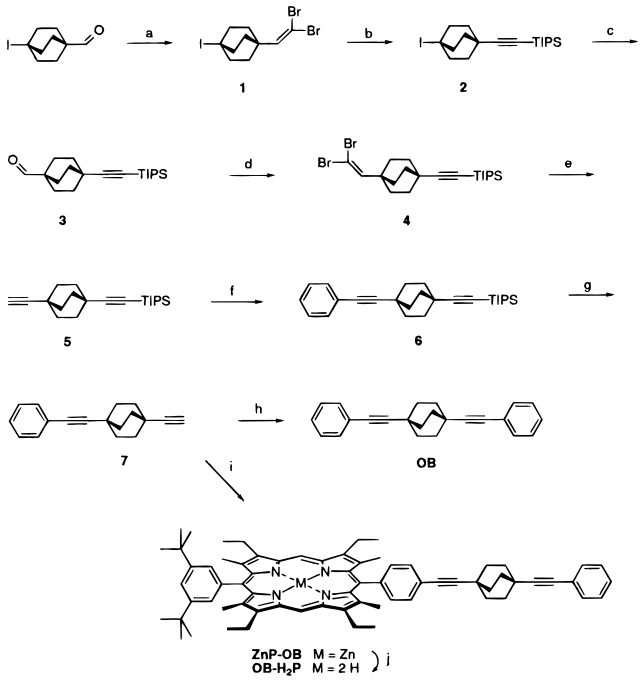

[a] (a) PPh_3, Zn, CBr_4, CH_2Cl_2; 89%; (b) BuLi, TIPSCl, THF; 52%; (c) *t*-BuLi, *N*-formylpiperidine, ether; 70%; (d) See Step A; 94%; (e) BuLi, THF; 92%; (f) PhI, $Pd(PPh_3)_4$, CuI, Piperidine; 96%; (g) Bu_4NF, THF, 79%; (h) See Step f; 94%; (i) **8**, Pd_2Dba_3•$CHCl_3$, PPh_3, PhMe/piperidine (1:1); 75%; (j) TFA, CH_2Cl_2; 93%.

SCHEME 2[a]

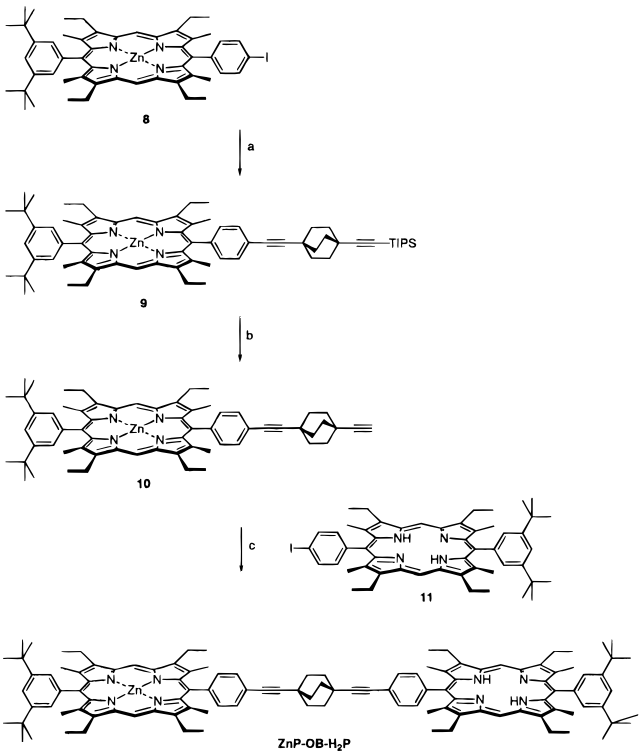

[a] (a) **5**, Pd_2Dba_3•$CHCl_3$, PPh_3, PhMe/Piperidine (1:1); 53%; (b) Bu_4NF, THF; 86%; Pd_2dba_3•$CHCl_3$, PPh_3, PhMe/piperidine (1:1); 40%.

bicyclo[2.2.2]octane (OB), were synthesized from building block **7** (Scheme 1).

The synthesis of the building block **5** went via 5-iodobicyclo-[2.2.2]octane-1-carbaldehyde[22] (Scheme 1), which was converted to dibromoalkene **1** by using the Corey-Fuchs' protocol.[23] The anion formed by treatment of **1** with butyllithium was reacted with chlorotriisopropylsilane (TIPS chloride) affording the silylated alkyne **2**. Aldehyde **3** was prepared from **2** by treatment with *tert*-butyllithium and *N*-formylpiperidine using the procedure of Olah et al.,[24] and finally the Corey-Fuchs' procedure was repeated to give the monosilylated diyne **5** via dibromoalkene **4**.

In the next step, bridge building block **5** was coupled with zinc iodoporphyrin **8**. The first attempt using the same conditions as in the preparation of arene-linked compounds, i.e., treatment with Pd_2dba_3•$CHCl_3$, $AsPh_3$ in toluene/triethylamine (3:1) at 40 °C,[21] was not successful. Under those conditions porphyrin **8** reacted with two molecules of **5**, probably forming an enyne-linked porphyrin derivative.[25] The effect of different amines on the Sonogashira coupling was studied by Linstrumelle and co-workers,[26] who showed that piperidine and pyrrolidine are far more effective than triethylamine. Based on their findings the triethylamine was replaced by piperidine. The porphyrin dimer ZnP−OB−H_2P could then be obtained in 17% yield in three steps from **5**, zinc iodoporphyrin **8**, and free base iodoporphyrin **11** (Scheme 2). Despite the higher reactivity in piperidine, the coupling reactions had to be performed at high temperature (70−80 °C) for 2−3 days because of the lower reactivity of alkylacetylenes compared with phenylacetylenes.[19]

Building block **7** was prepared from **5** by palladium-catalyzed coupling with iodobenzene under the conditions described by Alami et al.[26] followed by desilylation with tetrabutylammonium fluoride. The coupling with iodobenzene was repeated to give OB. The reference porphyrin ZnP−OB was prepared from **7** and zinc iodoporphyrin **8**. The use of PPh_3 instead of $AsPh_3$ in the preparation of ZnP−OB led to somewhat shorter reaction time (22 h at 70 °C) and the yield was improved compared with the coupling of zinc iodoporphyrin **8** with **5**. Demetalation[27] of ZnP−OB with trifluoroacetic acid gave OB−H_2P.

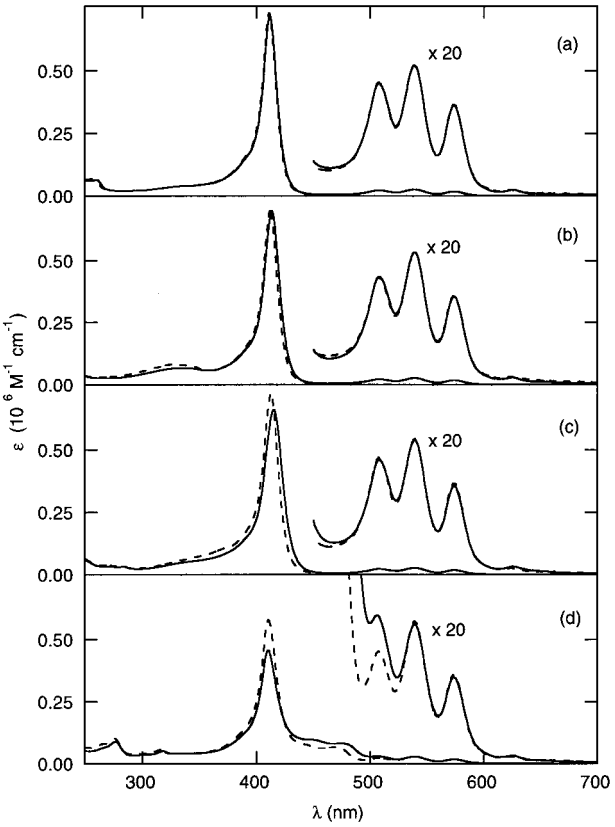

Figure 2. Absorption spectra of dimers (—) and the sum of absorption spectra of reference compounds (– – –) in $CHCl_3$, 20 °C. From top to bottom: (a) ZnP−OB−H2P and ZnP−OB + H_2P; (b) ZnP−BB−H_2P and ZnP−BB + H_2P; (c) ZnP−NB−H_2P and ZnP−NB + H_2P; (d) ZnP−AB−H_2P and ZnP−AB + H_2P.

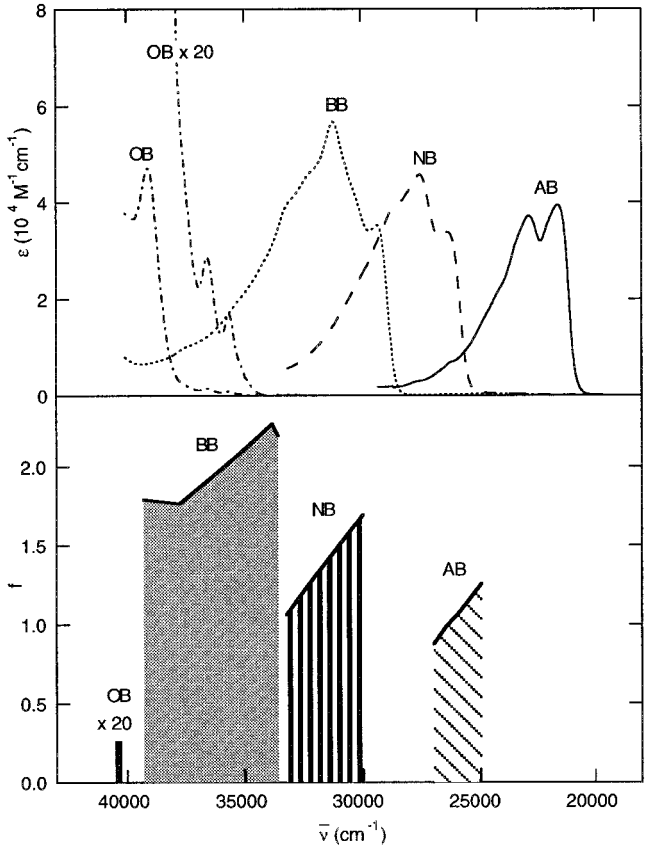

Figure 3. Top: Absorption spectra in the region of the first transition ($S_0 \rightarrow S_1$) in the bridging chromophores: AB (—), NB (– – –), BB (. . .), and OB (– · –) in $CHCl_3$, 20 °C. Bottom: Calculated $S_0 \rightarrow S_1$ excitation energies and oscillator strengths of different dihedral conformations of the bridging chromophores. See text for details.

Spectroscopic Properties. The identity of the separate chromophores (donor, bridge, acceptor) is preserved in the systems, which is seen by comparing the absorption spectra of the systems with the sum of spectra of the separate chromophores (Figure 2). The absorption spectra of ZnP−OB−H_2P, ZnP−BB−H_2P, and ZnP−NB−H_2P can be resolved into a 1:1:1 mixture of their components: ZnP/OB/H_2P, ZnP/BB/H_2P, and ZnP/NB/H_2P, respectively, or a 1:1 mixture of their reference compounds, either ZnP−RB/H_2P or ZnP/RB−H_2P (R = O, B, N). Similarly, the absorption spectrum of ZnP−AB−H_2P is the spectral sum of its components or reference compounds in the Q-band region (λ > 520 nm) but significant deviations are observed in the Soret bands ($\lambda \approx$ 410 nm) of the porphyrins (Figure 2d). In Figure 2 the spectral sum of ZnP−RB and H_2P is shown and compared with the spectra of ZnP−RB−H_2P. The major contribution to the absorption spectra of the D−B−A systems is from the porphyrin moieties. The same behavior is observed for the systems with ZnPpy as the donor (data not shown), but the spectrum of ZnPpy is red-shifted compared with that of ZnP, and the relative intensities of the Q-bands are changed.

The energies of the lowest singlet excited states are estimated from absorption spectra (Figure 3, top panel) and fluorescence spectra (not shown) of the separate chromophores. The energies are 35 000 cm^{-1}, 29 000 cm^{-1}, 26 000 cm^{-1}, and 21 300 cm^{-1} for the bicyclo[2.2.2]octane, benzene, naphthalene, and anthracene bridging chromophores, respectively. Calculations using INDO/S[28] on the geometry-optimized (PM3) bridging chromophores with varying dihedral angles yielded fairly good agreement with experimental data (Figure 3, lower panel). The experimental energies of the lowest singlet excited states of the bridging chromophores should be compared with the lowest singlet excitation energies of ZnP (17 400 cm^{-1}), ZnPpy (17 000 cm^{-1}), and H_2P (16 000 cm^{-1}). The excitation energy of the bridging chromophore is large enough in all systems to prevent stepwise energy transfer: D→B→A.

Förster Theory. For donor−acceptor pairs in which the electronic structure of the medium does not directly influence the energy transfer, the Förster theory can be used to describe long-range EET (D−A distances > 10 Å).[29] According to the Förster theory, the expected energy-transfer rate constant, $k_{EET}^{Förster}$, can be estimated from photophysical properties of the separate donor (ZnP or ZnPpy) and acceptor (H_2P) moieties

$$k_{EET}^{Förster} = 8.79 \times 10^{-25} (k_D \kappa^2 J / n^4 R^6)\ s^{-1} \quad (1)$$

The orientation factor, κ^2, is defined from unit vectors as[30]

$$\kappa^2 = ((\hat{\mu}_d \cdot \hat{\mu}_a) - 3(\hat{\mu}_d \cdot \hat{r})(\hat{r} \cdot \hat{\mu}_a))^2 = (\sin\theta \sin\omega \cos\phi - 2\cos\theta \cos\omega)^2 \quad (2)$$

where ω is the angle between the donor transition dipole moment (represented by the unit vector $\hat{\mu}_d$) and the (unit) vector ($\hat{r}$) connecting the donor and acceptor transition dipole moment; θ is the angle between the acceptor transition dipole moment (represented by the unit vector $\hat{\mu}_a$) and $\hat{r}$; and ϕ is the angle between the two porphyrin planes. Zinc 5,10,15,20-tetraphenyl porphyrin with D_{4h} symmetry has the lowest transition moments degenerated in the porphyrin plane.[31] Fluorescence anisotropy measurements on ZnP in a vitrified glass gave the anisotropy value 0.1 for all excitation wavelengths indicating that zinc 5,15-

diphenylporphyrin (and ZnPpy) also has the lowest transition moments effectively degenerated in the porphyrin plane ($0° \leq \omega \leq 360°$). Semiempirical calculations (INDO/S) showed that the first transition moment of the H_2P is along its N−N-axis, giving $\theta = 45°$, i.e., the angle expected for a D_{2h} symmetric free base porphyrin.[31] The value of κ^2 is then found to vary between 2/3 and 1 for the different configurations of the porphyrin planes and for the dynamic average $\kappa^2 = 5/6$.[30] Because of the small variance in κ^2, $k_{EET}^{Förster}$ will change only slightly for different conformations. For the present porphyrin dimers the calculated energy-transfer efficiency is independent of whether the dynamic or the static average is used.

As previously mentioned the donor−acceptor distance, R, is the same for all D−B−A systems in the two series and is estimated to be 25.3 Å. The refractive index of the solvent ($CHCl_3$), n, is 1.45.[32] The radiative rate constant, k_D, is calculated from the fluorescence quantum yield (ϕ_D) and the fluorescence lifetime (τ_D) of the donor in absence of acceptor; $k_D = \phi_D/\tau_D = 2.0 \pm 0.1 \times 10^7\ s^{-1}$ for ZnP and $k_D = 1.6 \pm 0.1 \times 10^7\ s^{-1}$ for ZnPpy. The spectral overlap integral, J, is calculated from the acceptor absorption spectrum ($\epsilon(\lambda)$) and the normalized donor emission spectrum ($F(\lambda)$) as

$$J = \int_0^\infty \epsilon(\lambda) F(\lambda) \lambda^4 d\lambda \qquad (3)$$

which gives $J = 2.6 \pm 0.2 \times 10^{-14}\ M^{-1}\ cm^{-3}$ for systems with ZnP as the donor and $J = 0.9 \pm 0.2 \times 10^{-14}\ M^{-1}\ cm^{-3}$ for systems with ZnPpy as the donor. The spectral overlap integral with ZnPpy as the donor is significantly smaller than with ZnP, because the emission spectrum of ZnPpy is red-shifted and the intensities of the Q-bands are altered (Figure 4). Within the Förster approximation, the expected EET rate constants are equal for all ZnP−RB−H_2P systems, $k_{EET}^{Förster} = 3.3 \pm 0.1 \times 10^8\ s^{-1}$, and for all ZnPpy−RB−$H_2P$ systems, $k_{EET}^{Förster} = 0.9 \pm 0.1 \times 10^8\ s^{-1}$.

Fluorescence Emission Spectra and Lifetimes. The measured EET rate constants of the systems differ from the values predicted by the Förster theory. The EET rate constants are calculated as

$$k_{EET} = \frac{E}{(1-E)\tau_0} \qquad (4)$$

where E is the EET efficiency (see Table 2). The efficiency is calculated from the steady-state or lifetime measurements as

$$E = 1 - \frac{I}{I_0} = 1 - \frac{\tau}{\tau_0} \qquad (5)$$

where I and I_0 are the donor emission intensities of the systems and of the 1:1 reference mixtures, respectively, and τ and τ_0 are the corresponding fluorescence lifetimes.

Figure 5a shows fluorescence emission spectra of ZnP−OB−H_2P, ZnP−BB−H_2P, ZnP−NB−H_2P, and ZnP−AB−H_2P, and of a 1:1 mixture of ZnP and H_2P. The fluorescence spectrum of ZnP is almost indistinguishable from the spectra of ZnP−RB (not shown). Figure 5b shows the fluorescence emission spectra of the corresponding ZnPpy−RB−H_2P systems and reference mixture. The donors dominate the emission between 550 and 600 nm (ZnP) or between 570 and 610 nm (ZnPpy), whereas the acceptor (H_2P) dominates the emission above 680 nm. The energy-transfer efficiencies were calculated from the decrease in intensity of the donor emission. Similar results were found by calculating E from the increase in acceptor emission. Figure 5 clearly shows that the donor emission decreases and the acceptor emission increases in the covalently linked porphyrin dimers when compared with the 1:1 reference mixture. The same trend of EET efficiencies: ZnP(py)−OB−H_2P < ZnP(py)−BB−H_2P < ZnP(py)−NB−H_2P < ZnP(py)−AB−H_2P is found in both series. However, the ZnPpy−RB−H_2P series shows less efficient EET than the ZnP−RB−H_2P series, which agrees with expectations from the Förster theory.

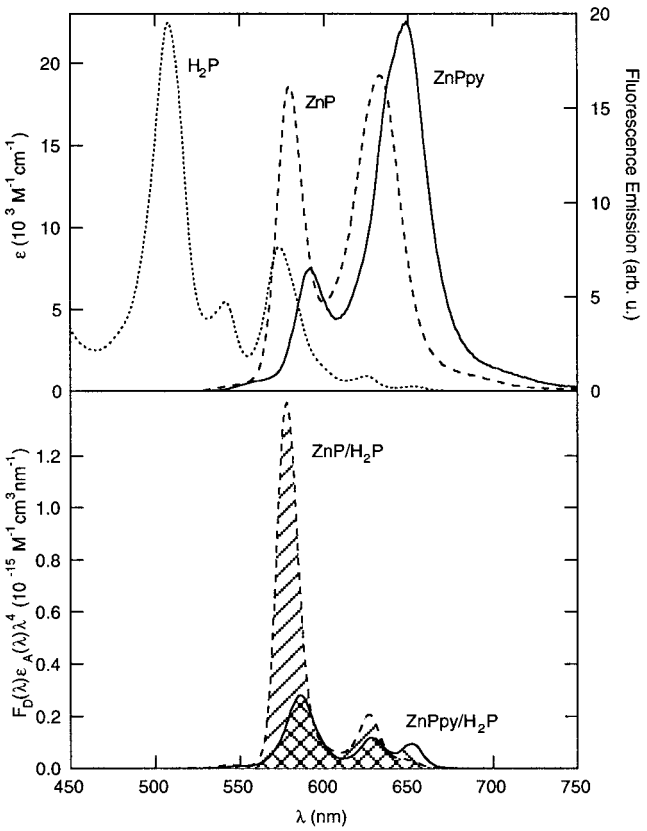

Figure 4. Top: Absorption spectrum of H_2P (. . .) and emission spectra of ZnP (− − −) and ZnPpy (—) in $CHCl_3$, 20 °C. On adding pyridine to ZnP the relative emission intensity of Q(1,0):Q(0,0) is changed from approximately 1:1 to 3:1. Bottom: The calculated spectral overlap between ZnP and H_2P (− − −, area //) and between ZnPpy and H_2P (—, area \\).

The fluorescence lifetimes of the reference compounds (ZnP−RB, ZnPpy−RB, and RB−H_2P) are, within experimental error, independent of the bridging chromophore connected to the porphyrin moiety. The lifetimes of ZnPpy−RB are a little shorter than that found for the corresponding ZnP−RB. In the D−B−A systems, fluorescence from both donor and acceptor is observed. In the analysis of the time-resolved data, the lifetime of the acceptor is fixed to the lifetime measured for RB−H_2P, and the donor lifetime is found from the best fit to the data points. The resulting lifetimes and fractions (f) of ZnP and ZnPpy emission are shown in Table 2. The lifetime of the donor in the reference compounds was compared with the donor lifetime in the D−B−A systems to calculate E.

Because the efficiencies from steady-state and time-resolved measurements are slightly different, a weighted average E-value was calculated. This E-value was used to calculate k_{EET}. The results clearly show that the rate constant for EET is highest in the systems with anthracene in the bridging chromophore. The systems with naphthalene or benzene in the bridging chromophore give a slightly higher rate constant than in the systems with bicyclo[2.2.2]octane in the bridging chromophore.

TABLE 2: Observed Donor Fluorescence Intensities (I), Donor and Acceptor Lifetimes (τ), Fraction of Donor Fluorescence Intensity in Lifetime Measurements (f), Calculated EET Efficiencies (E) and Rate Constants (k_{EET}) ($CHCl_3$ solutions at 20 °C)

compound	I, au	E	τ_{XB-H_2P},[a] ns	f_{ZnP}, %	τ_{ZnP}, ns	E	E[b]	k_{EET},[c] s^{-1}
ZnP−OB	41.3				1.29 ± 0.05			
ZnP−OB−H_2P	26.6	0.36 ± 0.04	8.52 ± 0.21	49	0.96 ± 0.05	0.26 ± 0.06	0.32	3.7×10^8
ZnP−BB	41.7				1.27 ± 0.04			
ZnP−BB−H_2P	24.7	0.41 ± 0.04	8.37 ± 0.23	43	0.84 ± 0.06	0.34 ± 0.06	0.38	4.8×10^8
ZnP−NB	40.6				1.26 ± 0.05			
ZnP−NB−H_2P	23.3	0.43 ± 0.04	8.48 ± 0.23	40	0.82 ± 0.05	0.35 ± 0.06	0.40	5.3×10^8
ZnP−AB	37.6				1.24 ± 0.04			
ZnP−AB−H_2P	13.5	0.64 ± 0.06	8.32 ± 0.25	26	0.55 ± 0.05	0.56 ± 0.06	0.60	12.1×10^8
ZnPpy−OB	14.4				1.21 ± 0.04			
ZnPpy−OB−H_2P	12.3	0.15 ± 0.02	8.52 ± 0.21	60	1.07 ± 0.06	0.12 ± 0.07	0.15	1.5×10^8
ZnPpy−BB	14.2				1.20 ± 0.04			
ZnPpy−BB−H_2P	10.6	0.25 ± 0.04	8.37 ± 0.23	46	0.92 ± 0.06	0.23 ± 0.07	0.25	2.8×10^8
ZnPpy−NB	14.3				1.20 ± 0.05			
ZnPpy−NB−H_2P	10.2	0.29 ± 0.04	8.48 ± 0.23	41	0.89 ± 0.05	0.26 ± 0.08	0.29	3.4×10^8
ZnPpy−AB	12.3				1.19 ± 0.07			
ZnPpy−AB−H_2P	5.6	0.54 ± 0.07	8.32 ± 0.25	19	0.66 ± 0.13	0.45 ± 0.13	0.53	9.5×10^8

[a] Lifetimes of acceptor reference compounds were fixed in the analysis of time-resolved dimer fluorescence. [b] Estimated efficiency based on the weighted average between the values from steady-state and time-resolved measurements. [c] Rate constant calculated from the estimated efficiency.

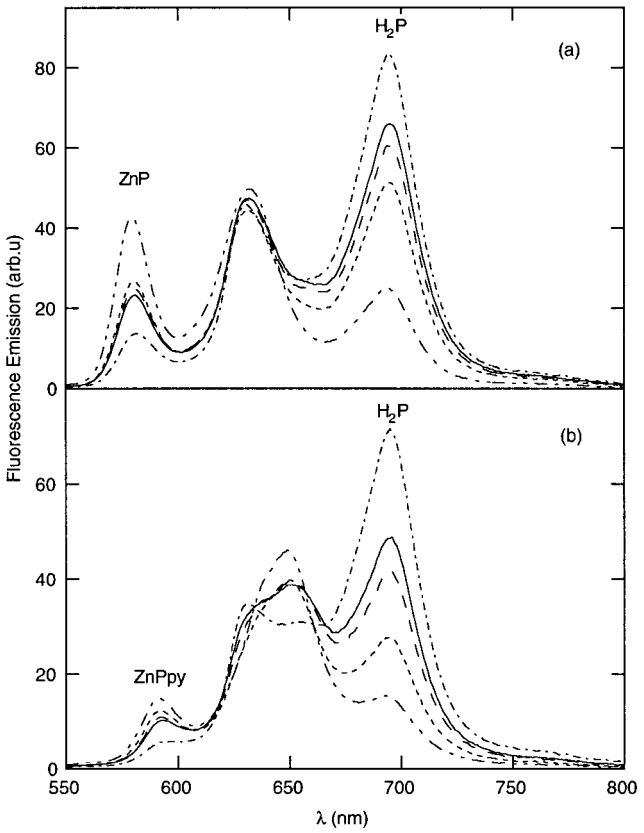

Figure 5. Fluorescence emission spectra of the dimers and a numerical 1:1 mixture of the reference compounds in $CHCl_3$, 20 °C. (a) ZnP:H_2P (− ·· −), ZnP−OB−H_2P (. . .), ZnP−BB−H_2P (− − −), ZnP−NB−H_2P (—) and ZnP−AB−H_2P (− · −). (b) ZnPpy:H_2P (− ·· −), ZnPpy−OB−H_2P (. . .), ZnPpy−BB−H_2P (− − −), ZnPpy−NB−H_2P (—), and ZnPpy−AB−H_2P (− · −).

Discussion

Structure. All systems studied are built from the same kind of building blocks. We therefore expect all the systems to behave similarly with respect to geometric parameters, and thus facilitate immediate comparison. The calculated length of the bridging chromophores (16.4 Å) was, within the expected error, neither dependent on the method used nor on the central unit in the bridging chromophore. Furthermore, the length was independent of the orientation of the central unit relative to the phenyl groups.

The calculations were done on linear bridging chromophores. From a high-field NMR study, Bothner-By et al. found that for a porphyrin dimer linked with diphenylethyne the out-of-plane bending could be as large as 26° for the entire dimer.[33] Our bridging chromophores have one more phenylethylene group in the linker, and in the worst case we could expect this linker to bend as much as the entire system of Bothner-By et al. For a bridging chromophore bend of 28°, the end-to-end distance was calculated to be 16.0 Å. The bending is assumed to be equal for all bridging chromophores. This large bending corresponds to an energy ≈2.7 kcal/mol higher than for the planar conformation as calculated by PM3. It is therefore not likely to be found at room temperature, and we believe that, even if the systems are slightly bent, this does not influence the donor−acceptor distance or the energy transfer significantly.

Calculations also showed that the dihedral angle between the plane of the central unit and the plane of the phenyl groups was distributed almost uniformly between 0° and 90° at room temperature. For OB no rotational barrier was found. In the other bridging chromophores the barriers for rotation of the central unit from $\alpha = 0°$ (central unit plane parallel to the plane of the phenyl groups) to $\alpha = 90°$ (central unit plane perpendicular to the plane of the phenyl groups) were small enough (<1 kcal/mol) to ensure the presence of all conformations at room temperature.

Spectroscopic Properties. The absorption spectra of all systems could be resolved numerically into equimolar contributions from the corresponding reference compounds. Figure 2 shows that the spectrum of ZnP−OB−H_2P is resolved perfectly in both the Soret and Q-band regions. Also, the Q-bands in the absorption spectra of ZnP−BB−H_2P and ZnP−NB−H_2P are equal to the sum of reference compounds. However, a small deviation is seen in the Soret bands: the deviation is larger for ZnP−NB−H_2P than for ZnP−BB−H_2P which is probably due to the first absorption band of NB being closer in energy to the Soret bands than the absorption of BB. For ZnP−AB−H_2P only the Q-bands could be described as a sum of the reference compounds. The significant deviation in the Soret band region is expected because, in the spectrum of ZnP−AB−H_2P, the Soret bands of the porphyrins overlap with the first absorption band of AB, making the situation for electronic coupling perfect.[34] A similar behavior was found for the absorption spectra of the systems with ZnPpy as donor. Therefore, in all fluorescence experiments an excitation wavelength in the Q-band

TABLE 3: Comparison of Measured Rate Constants for Energy Transfer and Rate Constants Expected from the Förster Theory

compound	k_{EET}, s^{-1}	$k_{EET}^{Förster}$, s^{-1}	mediating contribution,[a] k_{EET}^{Med}, s^{-1}	ΔE_{DB},[b] cm^{-1}
ZnP−OB−H_2P	3.7×10^8	3.3×10^8	0.4×10^8	17 600
ZnPpy−OB−H_2P	1.5×10^8	0.9×10^8	0.6×10^8	18 000
ZnP−BB−H_2P	4.8×10^8	3.3×10^8	1.5×10^8	11 600
ZnPpy−BB−H_2P	2.8×10^8	0.9×10^8	1.9×10^8	12 000
ZnP−NB−H_2P	5.3×10^8	3.3×10^8	2.0×10^8	8 600
ZnPpy−NB−H_2P	3.4×10^8	0.9×10^8	2.5×10^8	9 000
ZnP−AB−H_2P	12.1×10^8	3.3×10^8	8.8×10^8	3 900
ZnPpy−AB−H_2P	9.5×10^8	0.9×10^8	8.6×10^8	4 300

[a] $k_{EET}^{Med} = k_{EET} - k_{EET}^{Förster}$. [b] $\Delta E_{DB} = E_{bridge} - E_{donor}$.

region was selected, where the identity as independent chromophores of donor, bridge, and acceptor is preserved.

The energies of the lowest excited state of the bridging chromophores are found from the absorption (Figure 3) and fluorescence spectra (not shown). Figure 3 also shows the calculated energy (INDO/S) of the first absorption band for different rotations of the central unit in the bridging chromophore ($\alpha = 0°$, 15° ... 90°). These calculated excitation energies are in fair agreement with the observed spectra. They are calculated to be approximately 4000 cm^{-1} higher in energy than observed, but the relative energies agree well. The calculated intensities also agree with the observed spectra. For AB, NB, and BB the $S_0 \rightarrow S_1$ transition is of high intensity. In OB the first transition is due to exciton coupling[34] of the phenylethynyl groups, and it is calculated and observed to have low intensity. According to the experimental data the lowest excited singlet state of the bridging chromophores are approximately 4 000 cm^{-1} (AB), 8 000 cm^{-1} (NB), 12 000 cm^{-1} (BB), and 18 000 cm^{-1} (OB) higher in energy than the donor porphyrins. The separation is large enough to exclude stepwise energy transfer but the bridging chromophores do have some nontrivial effect on the EET, according to the obtained rate constants. Because AB is closest in energy to the donor and acceptor, we found the largest mediating effect for this bridging chromophore (vide infra).

The difference between the two series is related to the properties of the donor. The absorption and emission of ZnPpy is red-shifted approximately 10 nm, and the relative intensity of the two emission peaks is altered compared with the spectra of ZnP. This changes the spectral overlap significantly (Figure 4), and it is this change that makes the largest contribution to the decrease in Förster rate constant for the ZnPpy−RB−H_2P systems compared with the ZnP−RB−H_2P systems.

Mediation Contribution to Electronic Energy Transfer. Our results show that with anthracene as the central unit in the bridging chromophore the rate constant for singlet−singlet EET between the donor and the acceptor in the porphyrin dimers is significantly increased. Furthermore, the systems with benzene and naphthalene in the bridging chromophore showed a moderate increase in k_{EET}, whereas the systems with bicyclo[2.2.2]-octane as the central unit showed almost the k_{EET} expected from the Förster theory.

Table 3 shows the experimentally determined rate constants compared with the rate constants predicted from the Förster theory. In the fourth column of Table 3, the difference between measured (k_{EET}) and calculated ($k_{EET}^{Förster}$) rate constants is shown. If the difference for a specific ZnP−RB−H_2P system is compared with the difference for the corresponding ZnPpy−RB−H_2P system, it can be seen that these differences are essentially equal for each pair of porphyrin dimers with the same bridging chromophore. The difference varies with the electronic structure of the bridging chromophore, and is therefore a mediating effect specific for each bridging chromophore. The mediating effect is much higher for anthracene (8×10^8 s^{-1}) than for benzene or naphthalene (1.5 and 2×10^8 s^{-1}) in the bridging chromophore, whereas bicyclo[2.2.2]octane showed the smallest mediating effect (0.4×10^8 s^{-1}).

The increase in electronic coupling between the donor and acceptor, observed as an increased rate of EET, seems to be strongly correlated to the excitation energies of the bridging chromophores. According to the Fermi golden rule[35] the rate constant for a nonradiative process is proportional to the square of the total electronic coupling (H_{DA}^{tot}) between the initial and final state

$$k_{EET} = \frac{2\pi}{\hbar} \rho |H_{DA}^{tot}|^2 \qquad (6)$$

where ρ is the density of final states. For eq 6 to be valid it must be assumed that the electronic coupling is sufficiently weak, i.e., the donor relax vibrationally before the EET process takes place. Furthermore, the excitation energy must quickly dissipate in the acceptor states to avoid repopulation of the donor excited state.[36] This is presumably the case in the studied systems. The electronic coupling (H_{DA}^{tot}), relevant for EET, may be divided arbitrarily into a Förster-type coupling (dipole−dipole coupling) and a mediation contribution that involves the electronic states of the bridging chromophore. The mediating effect, observed as a contribution to the rate constant, is assumed to be proportional to the square of the electronic coupling associated with the mediation, H_{DA}^{Med}. This term may be subdivided into several different contributions as has been done by Scholes, Ghiggino, Paddon-Row, and co-workers.[9e,10b,c,37] However, the emphasis in their studies has been on non-π-electron bridging subunits with large separation between the donor and bridge excited states. The results therefore are not immediately applicable to our systems. It should be noted that the separation of the Förster and mediation contributions is not suggested to be based on a theoretical model, but is merely the simplest procedure to show how our empirical observations could be rationalized. A more thorough theoretical treatment and explicit molecular orbital calculations for the H_{DA}^{Med} matrix element will be presented elsewhere,[38] and we will limit the discussion in this paper to a qualitative analysis of the relative magnitude of H_{DA}^{Med} for the different bridging chromophores.

A simple approximation for the mediation contribution to the electronic coupling is expected to be given by perturbation theory[35] which predicts that H_{DA}^{Med} is proportional to the inverse energy splitting between the excited states of donor and bridging chromophores (ΔE_{DB}), giving

$$(k_{EET}^{Med})^{1/2} \propto H_{DA}^{Med} \propto \frac{1}{\Delta E_{DB}} \qquad (7)$$

In Figure 6 the square root of the contribution to the observed rate constant from the mediation effect, $(k_{EET}^{Med})^{1/2}$ is plotted against the inverse excitation energy difference for donor and bridging chromophore, ΔE_{DB}^{-1}, for the present D−B−A systems. A linear relation is indeed found, and the intercept is close to zero as expected for the infinite energy difference (i.e., no mediation effect). It is also seen in Figure 6 that the effect is much more pronounced for the bridging chromophore with anthracene as the central unit than for any of the other bridging

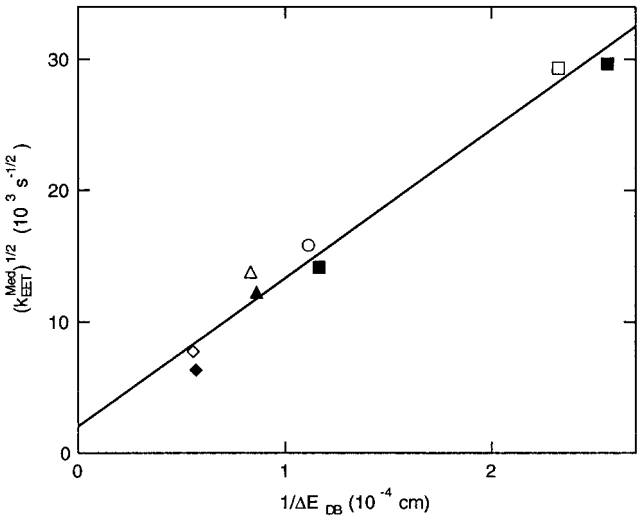

Figure 6. Linear plot of the square root of the mediating contribution $[(k_{EET}^{Med})^{1/2}]$ *versus* the reciprocal energy separation between the donor and the bridging chromophore (ΔE_{DB}^{-1}). Best linear fit (—), ZnP−OB−H_2P (◆), ZnPpy−OB−H_2P (◇), ZnP−BB−H_2P (▲), ZnPpy−BB−H_2P (△), ZnP−NB−H_2P (●), ZnPpy−NB−H_2P (○), ZnP−AB−H_2P (■), and ZnPpy−AB−H_2P (□).

chromophores. To clearly observe the mediating effect the energy splitting should not be too large, preferably $<6\ 000\ cm^{-1}$. On the other hand, the energy difference between bridging chromophore and donor excited states should not be smaller than the average thermal energy to avoid stepwise energy transfer (i.e., energy migration) becoming an important contribution to the overall EET rate. In this limit it might be very difficult to properly distinguish the mediation effect from simple migration behavior. This is, however, a very important situation because small energy gaps are an expected feature in most of the multichromophoric arrays for artificial and natural light-harvesting.

Conclusion and Remarks

In this investigation of EET in geometrically well-defined D−B−A systems the following conclusions were made: (1) The design of the present D−B−A systems allows the separation of bridging chromophore effects on the EET rate from other parameters known to govern energy transfer. (2) The electronic structure of the bridging chromophore, representing a medium between donor and acceptor, influences the EET rate. The bridging chromophore *mediates* electronic coupling. (3) The mediating contribution from the bridging chromophore can be separated from the total (observed) EET rates by comparison with the Förster theory. (4) The mediating contribution is correlated to the inverse energy splitting between excitation energies of the donor and bridging chromophores.

Work is in progress to perform molecular orbital calculations of the mediating matrix elements and to develop a theory for the mediating contribution. Furthermore, the corresponding ZnP−RB−Fe(III)P systems are currently being synthesized to investigate mediation effects on electron transfer.

Experimental Section

Synthesis. *Materials.* Diethyl ether, toluene, and tetrahydrofuran (THF) were dried by distillation from sodium/benzophenone under nitrogen. Dichloromethane and triethylamine were dried by distillation from calcium hydride under nitrogen. Dried solvents were used immediately after distillation. Piperidine (redistilled 99.5+ %) and other commercially available reagents were purchased from Aldrich and used without further purification.

Methods. Column chromatography of zinc porphyrins and porphyrin dimers was performed using silica gel (Merck, grade 60, 70−230 mesh). Flash chromatography was performed using silica gel (Matrex LC 60 Å/35−70 micron). Size exclusion chromatography (SEC) was performed using BioRad Bio-Beads S−X3 with toluene as eluent. ^{1}H (400 MHz) and ^{13}C (100.6 MHz) NMR spectra were recorded at room temperature with $CDCl_3$ as solvent, using a Varian UNITY-400 NMR spectrometer. Chemical shifts are reported relative to tetramethylsilane δ_H 0 ppm and $CDCl_3$ δ_C 77.0 ppm. Mass spectra were recorded using a VG ZabSpec instrument. Porphyrin-containing substances were analyzed by positive FAB-MS, other substances were analyzed by EI-MS (70 eV). Deaeration of reaction mixtures was performed by bubbling argon through the solution for 30 min. All palladium-catalyzed reactions were performed under argon atmosphere, palladium-catalyzed reactions involving porphyrins were performed in the dark.

1,1-Dibromo-2-(4-iodobicyclo[2.2.2]oct-1-yl)ethene (1). Triphenylphosphine (7.67 g, 29.2 mmol) and zinc powder (1.94 g, 29.7 mmol) were suspended in 80 mL of CH_2Cl_2 under argon. Carbon tetrabromide (9.69 g, 29.7 mmol) was added and the suspension was stirred at room temperature for 24 h. A solution of 4-iodobicyclo[2.2.2]octane-1-carbaldehyde[22a] in 20 mL of CH_2Cl_2 was added, and the mixture was stirred for an additional 24 h at room temperature. Hexane, 50 mL, was added and a brown precipitate was formed. The slurry was filtered through a pad of silica to remove insoluble material. The filtrate was evaporated to dryness and the residue was dissolved in 150 mL of ether. The solution was washed with 10% aqueous sodium bisulfite to remove traces of aldehyde, washed with water, dried (Na_2SO_4), and filtered. Evaporation of the solvent gave 5.48 g (89% yield) of a white solid. Recrystallization from pentane gave white crystals, mp 95−96 °C. ^{1}H NMR δ 1.96 (m, 6 H, $-CH_2CH_2-$), 2.47 (m, 6 H, $-CH_2CH_2-$), 6.32 (s, 1 H, $-CHCBr_2$); ^{13}C NMR δ 33.0, 33.4, 40.3, 44.0, 86.2, 144.8; HRMS Calcd for $C_{10}H_{13}Br_2I$: 417.843. Found: 417.839.

1-(Triisopropylsilyl)-2-(4-iodobicyclo[2.2.2]oct-1-yl)-ethyne (2). A solution of **1** (3.00 g, 7.14 mmol) in 50 mL of THF at −78 °C under argon was treated with *n*-butyllithium in hexanes (16 mmol, 10.1 mL of a 1.55 M solution). After being stirred for 1 h at −78 °C, the reaction mixture was allowed to reach room temperature and maintained for 1 h at that temperature. Chlorotriisopropylsilane (3.1 mL, 14 mmol) was added, and the reaction mixture was heated under reflux for 2 h. The reaction mixture was cooled to room temperature and water was added. The phases were separated and the aqueous layer was extracted with pentane. The combined organic layers were washed with water, dried (Na_2SO_4), filtered, and evaporated. Flash chromatography (silica gel, hexane) followed by bulb-to-bulb distillation (169−170 °C, 0.8 mbar) gave 1.54 g (52% yield) of a colorless oil. ^{1}H NMR δ 1.01 (m, 21 H, ^{i}Pr), 1.92 (m, 6 H, $-CH_2CH_2-$), 2.46 (m, 6 H, $-CH_2CH_2-$); ^{13}C NMR δ 11.1, 18.6, 25.0, 35.8, 40.2, 43.9, 80.1, 115.0; HRMS Calcd for $C_{19}H_{33}ISi$: 416.140. Found: 416.138.

4-[1-(Triisopropylsilyl)ethynyl]bicyclo[2.2.2]octane-1-carbaldehyde (3). A solution of **2** (1.54 g, 3.70 mmol) in 25 mL of ether at −100 °C under argon was treated dropwise with *tert*-butyllithium in pentane (7.7 mmol, 4.4 mL of a 1.76 M solution). The reaction mixture was warmed to −80 °C during 10 min and maintained for 5 min at that temperature. The reaction mixture was cooled to −100 °C, and *N*-formylpiperidine (5.7

mL, 51 mmol) was added dropwise. The reaction mixture was then allowed to reach room temperature and stirred for 30 min at that temperature. The reaction was quenched by addition of 10 mL of 2 M HCl. The phases were separated, and the aqueous layer was extracted with ether. The combined organic layers were washed with water, saturated aqueous $NaHCO_3$, and brine, dried (Na_2SO_4), filtered, and evaporated. Flash chromatography (silica, pentane/ether, 10:1) gave 0.82 g (70% yield) of a colorless oil. ^{1}H NMR δ 1.03 (m, 21 H, ^{i}Pr), 1.64 (m, 6 H, $-CH_2CH_2-$), 1.83 (m, 6 H, $-CH_2CH_2-$), 9.42 (s, 1 H, CHO); ^{13}C NMR δ 11.1, 18.6, 25.3, 28.2, 31.3, 42.7, 79.6, 115.3, 205.6; HRMS Calcd for $C_{20}H_{34}OSi$: 318.238. Found: 318.237.

1,1-Dibromo-2-[4-(1-(triisopropylsilyl)ethynyl)bicyclo[2.2.2]-oct-1-yl]-ethene (4). A solution of aldehyde **3** (0.75 g, 2.35 mmol) in 5 mL of CH_2Cl_2 was treated with PPh_3 (1.23 g, 4.70 mmol), zinc powder (0.31 g, 4.70 mmol), and CBr_4 (1.56 g, 4.70 mmol) suspended in 13 mL of CH_2Cl_2, using the same conditions as in the preparation of **1**. Hexane (20 mL) was added, and the resulting slurry was filtered through a pad of silica. The solvents were removed affording 1.05 g (94% yield) of colorless oil, which was used in the next step without further purification. ^{1}H NMR δ 1.02 (m, 21 H, ^{i}Pr), 1.80 (s, 12 H, $-CH_2CH_2-$), 6.40 (s, 1 H, $-CHCBr_2$); ^{13}C NMR δ 11.1, 18.6, 27.5, 29.5, 32.1, 35.2, 79.2, 85.5, 116.0, 145.6; HRMS Calcd for $C_{21}H_{34}Br_2Si$: 472.080. Found: 472.077.

[4-(1-(Triisopropylsilyl)ethynyl)bicyclo[2.2.2]oct-1-yl]-ethyne. (5). A solution of **4** (1.00 g, 2.10 mmol) in 15 mL of THF at -78 °C under argon was treated with *n*-butyllithium in hexanes (4.9 mmol, 3.6 mL of a 1.36 M solution). After being stirred at -78 °C for 1 h the reaction mixture was allowed to reach room temperature and maintained for 1 h at that temperature. Water was added and the phases were separated. The aqueous layer was extracted with pentane and the combined organic phases were washed with water, dried (Na_2SO_4), filtered, and evaporated. Flash chromatography (silica, pentane/ether, 50:1) gave 0.61 g (92% yield) of a colorless oil. ^{1}H NMR δ 1.02 (m, 21 H, ^{i}Pr), 1.78 (s, 12 H, $-CH_2CH_2-$), 2.08 (s, 1 H, CCH);^{13}C NMR δ 11.1, 18.6, 26.1, 26.9, 31.7, 31.8, 68.0, 79.4, 91.3, 115.7; HRMS Calcd for $C_{21}H_{34}Si$: 314.243. Found: 314.243; Anal. Calcd for $C_{21}H_{34}Si$: C 80.18; H 10.89. Found: C 79.99; H 11.04.

1-Phenyl-2-[4-(triisopropylsilylethynyl)bicyclo[2.2.2]oct-1-yl]ethyne (6). $Pd(PPh_3)_4$ (48 mg, 42 mmol) and CuI (16 mg, 84 mmol) were added under argon flushing to a deaerated solution of iodobenzene (224 mg, 1.1 mmol) and **5** (262 mg, 0.83 mmol) in 10 mL of piperidine. The reaction mixture was stirred for 30 min at room temperature. The solvent was removed under reduced pressure. The solid residue was suspended in pentane/ether (100:1) and added to a chromatographic column. Flash chromatography (silica, pentane/ether, 100:1) afforded the product containing traces of iodobenzene. The iodobenzene was removed by bulb-to-bulb distillation (120 °C, 4 mbar) leaving 311 mg (96% yield) of a colorless oil that crystallized upon cooling and scratching, mp 47−48 °C. ^{1}H NMR δ 1.03 (m, 21 H, ^{i}Pr), 1.83 (bs, 12 H, $-CH_2CH_2-$), 7.25 (m, 3 H, ArH), 7.35 (m, 2 H, ArH); ^{13}C NMR δ 11.2, 18.6, 26.8, 27.0, 31.8, 32.0, 79.3, 80.5, 96.5, 116.0, 123.8, 128.1, 131.5; HRMS Calcd for $C_{27}H_{38}Si$: 390.274. Found: 390.279.

[4-(Phenylethynyl)bicyclo[2.2.2]oct-1-yl]ethyne (7). Tetrabutylammonium fluoride (0.7 mmol, 0.6 mL of a 1.1 M solution in THF) was added to a solution of **6** (102 mg, 0.26 mmol) in 5 mL of THF under argon. The reaction mixture was stirred at room temperature for 90 min. Water was added and the phases were separated. The aqueous layer was extracted with ether and the combined organic layers were washed with water, dried (Na_2SO_4), filtered, and evaporated. Flash chromatography (silica, pentane/ether, 100:1) followed by sublimation (50 °C, 1 mbar) afforded 48 mg (79% yield) of white crystals, mp 89−90 °C. ^{1}H NMR δ 1.84 (m, 12 H, $-CH_2CH_2-$), 2.10 (s, 1 H, CCH), 7.25 (m, 3 H, ArH), 7.35 (m, 2 H, ArH); ^{13}C NMR δ 26.0, 26.7, 31.67, 31.70, 68.1, 80.6, 91.2, 96.2, 123.7, 127.5, 128.1, 131.5; HRMS Calcd for $C_{18}H_{18}$: 234.141. Found: 234.137; Anal. Calcd for $C_{18}H_{18}$: C 92.26; H 7.74. Found: C 92.31; H 7.79.

1,4-Bis(phenylethynyl)bicyclo[2.2.2]octane (OB). $Pd(PPh_3)_4$ (6 mg, 5 mmol) and CuI (2 mg, 10 mmol) were added under argon flushing to a deaerated solution of iodobenzene (29 mg, 0.14 mmol) and **7** (25 mg, 0.11 mmol) in 3 mL of piperidine. The reaction mixture was stirred for 30 min at room temperature and concentrated to dryness. The solid residue was suspended in pentane/ether (100:1) and added to a chromatographic column. Flash chromatography (silica, pentane/ether, 100:1) gave 32 mg (94% yield) of white crystals, mp 165−166 °C. ^{1}H NMR δ 1.89 (s, 12 H, $-CH_2CH_2-$), 7.26 (m, 6 H, ArH), 7.36 (m, 4 H, ArH); ^{13}C NMR δ 26.8, 31.8, 80.6, 96.4, 123.8, 127.5, 128.1, 131.5; HRMS Calcd for $C_{24}H_{22}$: 310.172. Found: 310.174; Anal. Calcd for $C_{24}H_{22}$: C 92.86; H 7.14. Found: C 92.70; H 7.10.

4-Phenylethynyl-1-{[zinc(II) 5-(3,5-di-*tert*-butylphenyl)-2,8,12,18-tetraethyl-3,7,13,17-tetramethyl-15-porphyrinyl]-phenylethynyl}bicyclo[2.2.2]octane (ZnP−OB). Pd_2dba_3•$CHCl_3$ (6 mg, 6 mmol) and PPh_3 (13 mg, 49 mmol) were added under argon flushing to a deaerated solution of zinc iodoporphyrin **8**[21] (38 mg, 41 mmol) and **7** (15 mg, 62 mmol) in 8 mL of toluene/piperidine (1:1). The reaction mixture was stirred for 22 h at 70 °C and concentrated to dryness. Chromatography (silica, pentane/CH_2Cl_2, 4:1 to pentane/CH_2Cl_2, 7:3) and SEC gave 32 mg (75% yield) of a red solid. ^{1}H NMR δ 1.51 (s, 18 H, *t*-Bu), 1.77 (m, 12 H, $-CH_2CH_3$), 2.01 (m, 6 H, $-CH_2CH_2-$), 2.08 (m, 6 H, $-CH_2CH_2-$), 2.44 (s, 6 H, pyrrole-CH_3), 2.49 (s, 6 H, pyrrole-CH_3), 4.00 (m, 8 H, $-CH_2CH_3$), 7.28 (m, 3 H, ArH), 7.41 (m, 2 H, ArH), 7.77 (dm, J = 8 Hz, 2 H, ArH), 7.81 (t, J = 1.8 Hz, 1 H, ArH), 7.93 (d, J = 1.8 Hz, 2 H, ArH), 8.00 (dm, J = 8 Hz, 2 H, ArH), 10.18 (s, 2 H, *meso*); HRMS Calcd for $C_{70}H_{76}N_4Zn$: 1036.536. Found: 1036.550.

4-Phenylethynyl-1-{free base porphyrinyl]phenylethynyl}-bicyclo[2.2.2]octane (OB−H_2P). The zinc porphyrin **ZnP−OB** (16 mg, 15 mmol) was dissolved in 10 mL of CH_2Cl_2. Trifluoroacetic acid (0.5 mL) was added, and the reaction mixture was stirred at room temperature for 1 h in the dark. The mixture was poured into ethyl acetate, washed with 5% aqueous $NaHCO_3$ until the reddish porphyrin color returned, washed with water, and dried (Na_2SO_4). The free base porphyrin was purified by chromatography on silica. Traces of zinc porphyrin were removed using CH_2Cl_2 and the free base porphyrin was then eluted by adding ether to the eluent. Removal of the solvents and drying in vacuo gave 14 mg (93% yield) of a brown solid. ^{1}H NMR δ −2.43 (bs, 2 H, NH), 1.50 (s, 18 H, *t*-Bu), 1.77 (m, 12 H, $-CH_2CH_3$), 2.01 (m, 6 H, $-CH_2CH_2-$), 2.07 (m, 6 H, $-CH_2CH_2-$), 2.46 (s, 6 H, pyrrole-CH_3), 2.53 (s, 6 H, pyrrole-CH_3), 4.02 (m, 8 H, $-CH_2CH_3$), 7.29 (m, 3 H, ArH), 7.41 (m, 2 H, ArH), 7.77 (dm, J = 8 Hz, 2 H, ArH), 7.80 (t, J = 1.8 Hz, 1 H, ArH), 7.91 (d, J = 1.8 Hz, 2 H, ArH), 8.00 (dm, J = 8 Hz, 2 H, ArH), 10.23 (s, 2 H, *meso*); FAB-MS Calcd for $C_{70}H_{78}N_4+H^+$: 974.6. Found: 974.5.

4-[(Triisopropylsilyl)ethynyl]-1-{[zinc(II) 5-(3,5-di-*tert*-butylphenyl)-2,8,12,18-tetraethyl-3,7,13,17-tetramethyl-15-porphyrinyl]phenylethynyl}bicyclo[2.2.2]octane (9). Pd_2dba_3•

$CHCl_3$ (9 mg, 8 mmol) and $AsPh_3$ (21 mg, 67 mmol) were added under argon flushing to a deaerated solution of zinc iodoporphyrin **8** (52 mg, 56 mmol) and **5** (21 mg, 76 mmol) in 16 mL of toluene/piperidine (3:1). The reaction mixture was stirred at 75 °C for 70 h and concentrated to dryness. Chromatography (silica, pentane/CH_2Cl_2, 4:1 to pentane/CH_2Cl_2, 1:1) gave 33 mg (53% yield) of a red solid. ^{1}H NMR δ 1.07 (m, 21 H, ^{i}Pr), 1.51 (s, 18 H, *t*-Bu), 1.76 (m, 12 H, $-CH_2CH_3$), 1.94 (m, 6 H, $-CH_2CH_2-$), 2.03 (m, 6 H, $-CH_2CH_2-$), 2.44 (s, 6 H, pyrrole-CH_3), 2.48 (s, 6 H, pyrrole-CH_3), 4.00 (m, 8 H, -CH_2CH_3), 7.75 (dm, J = 8 Hz, 2 H, ArH), 7.81 (t, J = 1.8 Hz, 1 H, ArH), 7.93 (d, J = 1.8 Hz, 2 H, ArH), 7.99 (dm, J = 8 Hz, 2 H, ArH), 10.17 (s, 2 H, *meso*); FAB-MS Calcd for $C_{73}H_{92}N_4SiZn$: 1116.638. Found: 1116.664.

4-Ethynyl-1-{[zinc(II) porphyrinyl]phenylethynyl}bicyclo-[2.2.2]octane (10). Tetrabutylammonium fluoride (105 mmol, 95 mL of a 1.1 M solution in THF) was added to a solution of **9** (38 mg, 35 mmol) in 10 mL of THF under argon. The reaction mixture was stirred for 1 h at room temperature, and the solvent was evaporated. The residue was dissolved in $CHCl_3$ and the solution was washed with saturated aqueous $NaHCO_3$, dried (Na_2SO_4), filtered, and evaporated. TLC (silica, pentane/ether, 10:1) and ^{1}H NMR indicated that the reaction was essentially complete. The product was purified by SEC to remove traces of **9** and residues of the protecting group. Removal of the solvent gave 24 mg (86% yield) of a red solid. ^{1}H NMR δ 1.51 (s, 18 H, *t*-Bu), 1.76 (m, 12 H, $-CH_2CH_3$), 1.93 (m, 6 H, $-CH_2CH_2-$), 2.04 (m, 6 H, $-CH_2CH_2-$), 2.14 (s, 1 H, CCH), 2.44 (s, 6 H, pyrrole-CH_3), 2.49 (s, 6 H, pyrrole-CH_3), 4.00 (m, 8 H, $-CH_2CH_3$), 7.75 (dm, J = 8 Hz, 2 H, ArH), 7.81 (t, J = 1.8 Hz, 1 H, ArH), 7.93 (d, J = 1.8 Hz, 2 H, ArH), 8.00 (dm, J = 8 Hz, 2 H, ArH), 10.18 (s, 2 H, *meso*); HRMS Calcd for $C_{64}H_{72}N_4Zn$: 960.505. Found: 960.508.

4-{5-(3,5-Di-*tert*-butylphenyl)-2,8,12,18-tetraethyl-3,7,13,17-tetramethyl-15-porphyrinyl]phenylethynyl}-1-{[zinc(II) 5-(3,5-di-*tert*-butylphenyl)-2,8,12,18-tetraethyl-3,7,13,17-tetramethyl-15-porphyrinyl]phenylethynyl}bicyclo[2.2.2]-octanne (ZnP−OB−H_2P). Pd_2dba_3•$CHCl_3$ (5 mg, 5 mmol) and $AsPh_3$ (12 mg, 40 mmol) were added under argon flushing to a deaerated solution of **10** (24 mg, 25 mmol) and free base iodoporphyrin **11**[21] (29 mg, 33 mmol) in 12 mL of toluene/piperidine (1:1). The reaction mixture was stirred at 80 °C for 60 h and concentrated to dryness. Chromatography (silica, CH_2Cl_2 to CH_2Cl_2/MeOH, 100:1) and SEC gave 17 mg (40% yield) of a red solid. ^{1}H NMR δ −2.43 (bs, 2 H, NH), 1.51 (s, 18 H, *t*-Bu), 1,52 (s, 18 H, t-Bu), 1.78 (m, 24 H, $-CH_2CH_3$), 2.19 (s, 12 H, $-CH_2CH_2-$), 2.44 (s, 6 H, pyrrole-CH_3), 2.46 (s, 6 H, pyrrole-CH_3), 2.53 (s, 6 H, pyrrole-CH_3), 2.55 (s, 6 H, pyrrole-CH_3), 4.02 (m, 16 H, $-CH_2CH_3$), 7.82 (m, 6 H, ArH), 7.92 (d, J = 1.8 Hz, 2 H, ArH), 7.93 (d, J = 1.8 Hz, 2 H, ArH), 8.04 (m, 4 H, ArH), 10.20 (s, 2 H, *meso*), 10.24 (s, 2 H, *meso*); HRMS Calcd for $C_{116}H_{132}N_8Zn$: 1700.987. Found: 1700.975.

Spectroscopic Measurements. All measurements were performed at 20 °C with amylene-stabilized $CHCl_3$ (Merck, HPLC grade) as the solvent.[39] Pyridine (LabScan) was distilled over KOH (BDH Chemicals) before use. ZnPpy, ZnPpy−RB, and ZnPpy−RB−H_2P were prepared directly before spectroscopic measurements by adding pyridine to the corresponding ZnP-solution. At a final pyridine concentration of approximately 2 M, full conversion of ZnP to ZnPpy was obtained, as judged from the changes in the absorption spectra.

Absorption spectra were recorded on a Cary 4 Bio spectrophotometer. Fully corrected steady-state emission spectra were recorded on a SPEX Fluorolog t2 spectrofluorimeter. To prevent aggregation of the samples, the concentration of the chromophores was kept at approximately 5 mM. The low concentration also excluded the possibility for intermolecular EET and that inner filter effects were negligible. Quantum yields were determined using rhodamine B in ethanol as reference (ϕ = 0.97[40]). The energy for the lowest singlet excited state was estimated for all chromophores from the midpoint between the maxima of the first transition observed in fluorescence and absorption spectra. To facilitate immediate comparison of the emission spectra of the D−B−A systems, the optical densities of the samples were matched at the excitation wavelength: 538 nm for ZnP samples and 550 nm for ZnPpy samples. The emission spectra of the reference mixtures were calculated from the numerical 1:1 mixture of the separate reference compounds. These "mixtures" were scaled to match the optical density of the dimers. The energy-transfer efficiency was calculated from the intensity of the donor emission at 580 nm for ZnP samples and at 592 nm for ZnPpy samples.

Fluorescence lifetimes were measured by the phase and modulation technique using a SPEX Fluorolog τ spectrofluorimeter. For the acceptor reference compounds (RB−H_2P) 20 modulation frequencies were selected on a logarithmic scale ranging from 2 to 200 MHz. The samples were excited at 507 nm and the emission was collected through a 550-nm cutoff filter. No change in lifetime with excitation wavelength was observed. For the donor reference compounds (ZnP−RB and ZnPpy−RB) and for the porphyrin dimers 20 modulation frequencies were selected on a logarithmic scale in ranging from 10 to 300 MHz. The emission was collected through a cutoff filter (550 nm for ZnP samples and 580 nm for ZnPpy samples), and the excitation wavelengths used were the same as in the steady-state measurements. In all time-resolved measurements a diluted silica sol scattering solution was used as the reference. For all reference compounds the observed demodulations and phase shifts could be fitted to a single-exponential model. For the dimers the data were fitted to a biexponential model. One component, corresponding to the relevant acceptor reference, RB−H_2P, was kept constant at the value determined from the pure reference compound. The other component was interpreted as the donor fluorescence decay. The goodness-of-fit was evaluated by the value of χ^2 and by visual inspection of the fit to the data points.

The fractions of donor fluorescence was calculated as $f = (\alpha_D\tau_D)/(\alpha_D\tau_D + \alpha_A\tau_A)$ where the α's are the preexponential factors and τ_D and τ_A are the lifetimes of donor and acceptor, respectively.

Quantum Mechanical Calculations. Because of the large size of our D−B−A systems we chose molecular mechanics calculations for estimation of the porphyrin center-to-center distance. The calculation was done with the force-field MM+[16] as implemented in the program package HyperChem.[41]

The semiempirical method PM3[17] was used to geometry optimize and calculate the potential energy of H_2P with different dihedral angles between phenyl and porphyrin planes. The calculations were performed in the program package MOPAC 6.0.[42] The angle for the first transition moment of H_2P was estimated using an INDO/S[28] calculation on the PM3 optimized structure.

For the bridging chromophores both semiempirical (AM1[43] or PM3,[17] HyperChem[41]) and ab initio (HF/3-21G*,[18] Gaussian 94[44]) methods were used in geometry optimizations and calculations of the potential energy surface for rotation of the central unit.

Acknowledgment. This work was supported by grants from the Swedish Natural Science Research Council (NFR), the Swedish Research Council for Engineering Sciences (TFR), and the Carl Trygger Foundation. K.K. is grateful to the Danish Research Academy for a fellowship. We thank Dr. Gunnar Stenhagen for performing the mass spectrometry measurements.

References and Notes

(1) *Antennas and Reaction Centers in Photosynthetic Bacteria*; Michel-Beyerle, M. E., Ed.; Springer-Verlag: New York, 1985. (b) McDermott, G.; Prince, S. M.; Freer, A. A.; Hawthornthwaite-Lawless, A. M.; Papiz, M. Z.; Cogdell, R. J.; Isaacs, N. W. *Nature* **1995**, *374*, 517−521. (c) Huber, R. *Angew. Chem., Int. Ed. Engl.* **1989**, *28*, 848−869. (d) van Grondelle, R.; Dekker: J. P.; Gillbro, T.; Sundström, V. *Biochim. Biophys. Acta* **1994**, *1187*, 1−65.

(2) (a) Wasielewski, M. R. *Chem. Rev.* **1992**, *92*, 435−461. (b) Kurreck, H.; Huber, M. *Angew. Chem., Int. Ed. Engl.* **1995**, *34*, 849−866. (c) Steinberg-Yfrach, G.; Rigaud, J.-L.; Durantini, E. N.; Moore, A. L.; Gust, D.; Moore, T. A. *Nature* **1998**, *392*, 479−482.

(3) (a) Wagner, R. W.; Lindsey, J. S.; Seth, J.; Palaniappan, V.; Bocian, D. F. *J. Am. Chem. Soc.* **1996**, *118*, 3996−3997. (b) Balzani, V.; Scandola, F. *Supramolecular Chemistry*; Ellis Horwood: Chichester, UK, 1991; Chapter 12.

(4) For reviews see: (a) Speiser, S. *Chem. Rev.* **1996**, *96*, 1953−1976. (b) Sauvage, J.-P.; Collin, J.-P.; Chambron, J.-C.; Guillerez, S.; Coudret; C.; Balzani, V.; Barigelletti, F.; De Cola, L.; Flamigni, L. *Chem. Rev.* **1994**, *94*, 993−1019.

(5) Newton, M. D. *Chem. Rev.* **1991**, *91*, 767−792.

(6) (a) Closs, G. L.; Piotrowiak, P.; MacInnis, J. M.; Fleming, G. R. *J. Am. Chem. Soc.* **1988**, *110*, 2652−2653. (b) Closs, G. L.; Johnson, M. D.; Miller, J. R.; Piotrowiak, P. *J. Am. Chem. Soc.* **1989**, *111*, 3751−3753.

(7) (a) Paddon-Row, M. N. *Acc. Chem. Res.* **1982**, *15*, 245−251. (b) Paddon-Row, M. N. *Acc. Chem. Res.* **1994**, *27*, 18−25.

(8) Hoffmann, R.; Imamura, A.; Hehre, W. J. *J. Am. Chem. Soc.* **1968**, *90*, 1499−1509.

(9) (a) Kroon, J.; Oliver, A. M.; Paddon-Row: M. N.; Verhoeven, J. W. *J. Am. Chem. Soc.* **1990**, *112*, 4868−4873. (b) Ghiggino, K. P.; Yeow, E. K. L.; Haines, D. J.; Scholes, G. D.; Smith, T. A. *J. Photochem. Photobiol. A* **1996**, *102*, 81−86. (c) Grosshenny, V.; Harriman, A.; Hissler, M.; Ziessel, R. *J. Chem. Soc., Faraday Trans.* **1996**, *92*, 2223−2238. (d) Scholes, G. D.; Ghiggino, K. P.; Oliver, A. M.; Paddon-Row: M. N. *J. Am. Chem. Soc.* **1993**, *115*, 4345−4349. (e) Scholes, G. D.; Ghiggino, K. P.; Oliver, A. M.; Paddon-Row, M. N. *J. Phys. Chem.* **1993**, *97*, 11871−11876. (f) Oevering, H.; Verhoeven, J. W.; Paddon-Row: M. N.; Cotsaris, E. *Chem. Phys. Lett.* **1988**, *143*, 488−495.

(10) (a) Lin, S. H.; Riao, W. Z.; Dietz, W. *Phys. Rev. E* **1993**, *47*, 3698−3706. (b) Scholes, G. D.; Ghiggino, K. P. *J. Chem. Phys.* **1995**, *103*, 8873−8883. (c) Clayton, A. H. A.; Scholes, G. D.; Ghiggino, K. P.; Paddon-Row, M. N. *J. Phys. Chem.* **1996**, *100*, 10912−10918.

(11) (a) McConnel, H. M. *J. Chem. Phys.* **1961**, *35*, 508−515. (b) Larsson, S. *J. Am. Chem. Soc.* **1981**, *103*, 4034−4040.

(12) (a) Osuka, A.; Yamada, H.; Maruyama, K.; Mataga, N.; Asahi, T.; Ohkouchi, M.; Okada, T.; Yamazaki, I.; Nishimura, Y. *J. Am. Chem. Soc.* **1993**, *115*, 9439−9452. (b) Seth, J.; Palaniappan, V.; Johnson, T. E.; Prathapan, S.; Lindsey, J. S.; Bocian, D. F. *J. Am. Chem. Soc.* **1994**, *116*, 10578−10592. (c) Osuka, A.; Tanabe, N.; Kawabata, S.; Yamazaki, I.; Nishimura, Y. *J. Org. Chem.* **1995**, *60*, 7177−7185. (d) Hsiao, J.-S.; Krueger, B. P.; Wagner, R. W.; Johnson, T. E.; Delaney, J. K.; Mauzerall, D. C.; Fleming, G. R.; Lindsey, J. S.; Bochian, D. F.; Donohoe, R. J. *J. Am. Chem. Soc.* **1996**, *118*, 11181−11193. (e) Seth, J.; Palaniappan, V.; Wagner, R. W.; Johnson, T. E.; Lindsey, J. S.; Bocian, D. F. *J. Am. Chem. Soc.* **1996**, *118*, 11194−11207. (f) Barigelletti, F.; Flamigni, L.; Collin, J.-P.; Sauvage, J.-P. *Chem. Commun.* **1997**, 333−338. (g) Vollmer, M. S.; Würthner, F.; Effenberger, F.; Emele, P.; Meyer, D. U.; Stümpfig, T.; Port, H.; Wolf, H. C. *Chem. Eur. J.* **1998**, *4*, 260−269.

(13) (a) Kawabata, S.; Yamazaki, I.; Nishimura, Y.; Osuka, A. *J. Chem. Soc., Perkin Trans. 2* **1997**, 479−484. (b) Strachan, J.-P.; Gentemann, S.; Seth, J.; Kalsbeck, W. A.; Lindsey, J. S.; Holten, D.; Bocian D. F. *J. Am. Chem. Soc.* **1997**, *119*, 11191−11201. (c) Gust, D.; Moore, T. A.; Moore, A. L. *Acc. Chem. Res.* **1993**, *26*, 198−203. (d) Gust, D.; Moore, T. A.; Moore, A. L.; Devadoss, C.; Lidell, P. A.; Hermant, R.; Nieman, R. A.; Demanche, L. J.; DeGraziano, J. M.; Gouni, I. *J. Am. Chem. Soc.* **1992**, *114*, 3590−3603.

(14) Craig, D. P.; Thiruamchandran, T. *Chem. Phys.* **1989**, *135*, 37−48.

(15) Jensen, K. K., van Berlekom, S. B., Kajanus, J., Mårtensson, J., Albinsson, B. *J. Phys. Chem. A* **1997**, *101*, 2218−2220.

(16) Allinger, N. L. *J. Am. Chem. Soc.* **1977**, *99*, 8127−8134.

(17) Stewart, J. J. P. *J. Comput. Chem.* **1989**, *10*, 209−220.

(18) (a) Gordon, M. S.; Binkley, J. S.; Pople, J. A.; Pietro, W. J.; Hehre, W. J. *J. Am. Chem. Soc.* **1982**, *104*, 2797−2803. (b) Binkley, J. S.; Pople, J. A.; Hehre, W. J. *J. Am. Chem. Soc.* **1980**, *102*, 939−947. (c) Pietro, W. J.; Francl, M. M.; Hehre, W. J.; DeFrees, D. J.; Pople, J. A.; Binkley, J. S. *J. Am. Chem. Soc.* **1982**, *104*, 5039−5048.

(19) (a) Cassar, L. *J. Organomet. Chem.* **1975**, *93*, 253−257. (b) Dieck, H. A.; Heck, F. R. *J. Organomet. Chem.* **1975**, *93*, 259−263. (c) Sonogashira, K.; Tohda, Y.; Hagihara, N. *Tetrahedron Lett.* **1975**, 4467−4470.

(20) Wagner, R. W.; Johnson, T. E.; Li, F.; Lindsey, J. S., *J. Org. Chem.* **1995**, *60*, 5266−5273.

(21) Kajanus, J.; van Berlekom, S. B.; Mårtensson, J.; Albinsson, B. *Synthesis*, in press.

(22) (a) Adcock, W.; Kok G. B. *J. Org. Chem.* **1985**, *50*, 1079−1087. (b) Adcock, W.; Abeywickrema, A. N. *J. Org. Chem.* **1982**, *47*, 2951−2957. (c) Grob, C. A.; Rich, R. *Helv. Chim. Acta* **1979**, *62*, 2802−2816.

(23) Corey, E. J.; Fuchs, P. L. *Tetrahedron Lett.* **1972**, 3769−3772.

(24) Olah, G. A.; Arvanaghi, M. *Angew. Chem., Int. Ed. Engl.* **1980**, *20*, 878−926.

(25) ^{1}H NMR δ 6.58 (s) in ratio of 1:2 to the meso protons. FAB-MS $C_{94}H_{126}N_4Si_2Zn$ Calcd. monoisotopic mass 1431. Found 1431.

(26) Alami, M.; Ferri, F.; Linstrumelle, G. *Tetrahedron Lett.* **1993**, *34*, 6403−6406.

(27) Lindsey, J. S.; Prathapan, S.; Johnson, T. E.; Wagner, R. W. *Tetrahedron* **1994**, *50*, 8941−8968.

(28) (a) Ridley, J.; Zerner, M. C. *Theor. Chim. Acta* **1973**, *32*, 111−134.

(29) (a) Förster, T. *Naturwissenschaften* **1946**, *33*, 166−175. (b) Förster, T. *Ann. Phys.* **1948**, *2*, 55−73.

(30) Dale, R.; Eisinger, J. Polarized Excitation Energy Transfer. In *Biochemical Fluorescence: Concepts*; Chen, R. F.; Edelhoch, H., Eds.; Marcel Dekker: New York, 1975; pp 115−284.

(31) Gouterman, M. Optical Spectra and Electronic Structure of Porphyrins and Related Rings. In *The Porphyrins*; Dolphin, D., Ed.; Academic Press: New York, 1978; Vol. III, pp 1−165.

(32) *Handbook of Chemistry and Physics*, 75th ed.; Lide, D. R., Ed.; CRC Press: Boca Raton, FL, 1995.

(33) Bothner-By, A. A.; Dadok, J.; Johnson, T. E.; Lindsey, J. S. *J. Phys. Chem.* **1996**, *100*, 17551−17557.

(34) Kasha, M. Energy Transfer, Charge Transfer, and Proton Transfer in Molecular Composite Systems. In *Physical and Chemical Mechanisms in Molecular Radiation Biology*; Glass, W. A.; Varma, M. N., Eds.; Plenum Press: New York, 1991; pp 231−255.

(35) Steinfeld, J. I. *Molecules and Radiation*; The MIT Press: Cambridge, MA, 1985.

(36) Reimers, J. R.; Hush, N. S. *Chem. Phys.* **1989**, *134*, 323−354.

(37) Harcourt, R. D.; Ghiggino, K. P.; Scholes, G. D.; Speiser, S. *J. Chem. Phys.* **1996**, *105*, 1897−1901.

(38) Kilså, K.; Mårtensson, J.; Larsson, S.; Albinsson, B., unpublished material.

(39) Please note that in the previous preliminary report CH_2Cl_2 was used as the solvent.

(40) Weber, G.; Teale, F. W. J. *Trans. Faraday Soc.* **1957**, *53*, 646−655.

(41) *HyperChem* (version 5), HyperCube, Inc., 1115 NW 4th Street, Gainesville, FL 32601, USA.

(42) *MOPAC 6.0* Program 455, Quantum Chemistry Program Exchange.

(43) Dewar, M. J. S.; Zoebish, E. G.; Healy, E. F.; Stewart, J. J. P. *J. Am. Chem. Soc.* **1985,** *107*, 3902−3909.

(44) *Gaussian 94*, Revision B.3, Frisch, M. J.; Trucks, G. W.; Schlegel, H. B.; Gill, P. M. W.; Johnson, B. G.; Robb, M. A.; Cheeseman, J. R.; Keith, T.; Petersson, G. A.; Montgomery, J. A.; Raghavachari, K.; Al-Laham, M. A.; Zakrzewski, V. G.; Ortiz, J. V.; Foresman, J. B.; Peng, C. Y.; Ayala, P. Y.; Chen, W.; Wong, M. W.; Andres, J. L.; Replogle, E. S.; Gomperts, R.; Martin, R. L.; Fox, D. J.; Binkley, J. S.; Defrees, D. J.; Baker, J.; Stewart, J. P.; Head-Gordon, M.; Gonzalez, C.; Pople, J. A.; Gaussian Inc.: Pittsburgh, PA, 1995.